

THE NATURE OF THE BOND-LENGTH CHANGE UPON MOLECULE COMPLEXATION

Weizhou WANG¹, Yu ZHANG and Baoming Ji^{2,*}

College of Chemistry and Chemical Engineering, Luoyang Normal University,
Luoyang 471022, China; e-mail: ¹wzwanglab@yahoo.com, ²lyhxjbm@126.com

Received October 26, 2009

Accepted December 9, 2009

Published online March 4, 2010

The nature of the bond-length change upon molecule complexation has been investigated at the MP2/aug-cc-pVTZ level of theory. Our results have clearly shown that the X-Y bond-length change upon complex formation is determined mainly by the electrostatic attractive interaction and the charge-transfer interaction. In the case of strongly polar bond, the electrostatic interaction always causes bond elongation while in the case of weakly polar bond it causes bond contraction. The charge-transfer interaction generally results in the X-Y bond elongation; either it is a more polar bond or it is a less polar bond. Employing this simple "electrostatic interaction plus charge-transfer interaction" explanation, we explained and predicted many interesting phenomena related to the bond-length change upon molecule complexation. In addition, the difference between the origin of the bond-length change upon hydrogen-bonded complex formation and the origin of the bond-length change upon halogen-bonded complex formation was also discussed.

Keywords: Bond-length change; Hydrogen bond; Halogen bond; Electrostatic interaction; Charge-transfer interaction; *Ab initio* calculations.

Molecular association and assembly are ubiquitous in nature, controlling virtually the properties of crystal, liquid and gas phases of many substances, and also metastable states. Formation of the molecular complex results in the change in the properties of the isolated molecule. For example, the formation of a hydrogen-bonded complex is always accompanied by a X-H bond elongation or contraction and a concomitant decrease or increase of the X-H stretch vibration frequency compared to the isolated species¹⁻¹³, so do the halogen-bonded complex and the lithium-bonded complex¹⁴⁻¹⁷. The study of the bond-length change and the concomitant spectral shift is important because this is the basis for several spectroscopic, structural, and thermodynamic techniques for the detection and investigation of molecular complex and it also plays a key role for the understanding of the nature of molecular interaction.

For the origin of the bond-length change upon hydrogen-bonded complex formation, there are mainly four different explanations: The first one attributes the X–H bond contraction to the negative dipole moment derivative of the proton donor^{2,5}. Schlegel, Li and Liu, however, suggested that the Pauli repulsion between two fragments leads to compression of the X–H bond and the orbital interactions cause X–H bond elongation⁴. The third explanation is based on the Bent's rule: Alabugin and co-workers concluded that it is the subtle balance of hyperconjugation and rehybridization that determines the X–H bond-length change⁷. In a very recent paper¹¹, Jemmis and Joseph proposed a new explanation for the X–H bond-length change in hydrogen bond. They argued that it is a net gain of electron density at the X–H bond region that causes an X–H bond contraction and the electrostatic interaction between the positive H and the negative Y forces an X–H bond elongation¹¹. Besides the hydrogen bond, there are also other important noncovalent interactions such as the halogen bond and the lithium bond^{14–18}. The explanations for the bond-length change upon the halogen-bonded complex are very similar to those for the hydrogen-bonded complex since extensive studies showed that many properties of the halogen bond are in parallel with those of the hydrgeon bond^{15,16,18}. Although these studies have identified many of the important aspects of the nature of the bond-length change upon molecule complexation, none of them are general enough to be applied across all the evidence and observations available so far^{1–17}, so it should be fair to say that the nature of the bond-length change upon molecule complexation is still not well understood.

The hydrogen bond and the halogen bond were for some time thought to result from the electrostatic attractive interaction. Later, the hydrogen-bonded complexes and the halogen-bonded complexes were classified as the charge-transfer complexes in which the charge-transfer is thought to be the dominant factor to determine the supramolecular structure. It is now recognized that, either for the hydrogen bond or for the halogen bond, the electrostatic effect, polarization, charge transfer, and dispersion contributions all play an important role; even so the importance of the electrostatic interaction and the charge-transfer interaction and their crucial roles in the molecular interaction are still prominent. In the present study, the nature of the X–Y bond-length change upon the X–Y…Z complexes (Y = H, Cl, Br, ...; Z = region of high electron density) formation has been revisited theoretically. We mainly focused on the role of the electrostatic attractive interaction and the charge-transfer interaction in the X–Y bond-length change upon the X–Y…Z complexes formation. It is not difficult to understand that in the negative electric field region of the electron donor Z, an

electron-rich, strongly polar bond always shows elongation, whereas an electron-poor, weakly polar bond is generally contracted. However, such a simple electrostatic interaction cannot explain the elongation of the weakly polar bond upon molecule complexation. As two molecules approach each other from a distance, the molecular orbitals begin to overlap until the equilibrium structure of a complex is attained. Usually, the overlaps occur between the X–Y σ^* antibonding orbital and the molecular orbital in the electron-rich region of Z, such as the lone-pair orbital, which leads to an electron density transfer from the electron-rich orbital to the X–Y σ^* antibonding orbital. The electron density transfer to the X–Y σ^* antibonding orbital causes a weakening of the X–Y bond followed by its elongation. Is it the charge-transfer interaction that tunes the X–Y bond-length change upon molecule complexation? If so, is the “electrostatic interaction plus charge-transfer interaction” explanation general and useful? These are two important questions that will be answered in this paper.

METHODS

It has been shown that the X–Y bond-length change upon complex formation is quite dependent on the computational method⁹. Electron correlation calculations with extended basis sets are thus required for the study of the bond-length change upon complex formation. In the present study, unless otherwise noted, structures of the monomers and dimers were determined at the second-order Møller–Plesset (MP2) theory level with the Dunning’s correlation consistent aug-cc-pVTZ basis set. The Gaussian 03 suite of programs was used for the structural optimizations¹⁹.

The natural bond orbital (NBO) theory of Weinhold and co-workers²⁰ was employed to calculate the orbital energy and to quantitatively evaluate the charge transfer from the electron-rich orbital of Z to the X–Y σ^* antibonding orbital. NBO analysis used the MP2-optimized structures, the Hartree–Fock (HF) densities, and the built-in subroutines of the Gaussian 03 program.

RESULTS AND DISCUSSION

The Role of the Electrostatic Interaction in the Bond-Length Change upon Molecule Complexation

In a strongly polar bond X–Y, X is always negatively charged and Y is positively charged, whereas in an electron-poor, weakly polar bond X–Y both X

and Y are always positively charged. According to the basic electrostatic principle, in the negative electric field region of the electron donor Z, the strongly polar bond should be elongated and the electron-poor, weakly polar bond will be contracted. Table I lists the X–Y bond-length change upon complex X–Y...Cl[−] formation. The distance between Y and Cl[−] is kept constant at 7.0 Å in order to eliminate the effect of the short-range interactions on the bond-length change. So the X–Y bond-length change can be approximately regarded as being caused only by the long-range electrostatic interaction. It can be seen from Table I that the strongly polar bonds O–Y, N–Y, F–Y, Cl–Y, and Br–Y are all elongated and the weakly polar bonds C–Y, P–Y and Si–Y are all contracted in the negative electric field region of the electron donor Cl[−], which is in good agreement with the above claim for the role of the electrostatic interaction in the bond-length change upon molecule complexation. In Table I, it can be also seen that the absolute value of the C–Cl contraction shows a systematic increase with the increasing number of F substituents. For the C–H and C–Br bonds, however, trisubstitution leads to a smaller contraction than disubstitution. Moreover, it has also been noticed that the magnitude of the C–Cl(Br) contraction is larger than that of the C–H contraction.

Table I also lists the O–H bond-length change upon the complex HO–H...H⁺ formation. The contraction of the O–H bond indicates that the strongly polar bond will be contracted and the weakly polar bond will be elongated in the positive electric field region. In a previous study, the O–H and N–H bond lengths were found to decrease slightly from those of the free molecules after encapsulating H₂O and NH₃ in a C₆₀ fullerene cage²¹. This can be explained as a result of the electrostatic interaction because inside the cage are all positive electrostatic potential regions²².

If the bond-length change upon molecule complexation is determined by the electrostatic interaction and the charge-transfer interaction, then it is impossible for the strongly polar bond to be contracted upon complex formation. In fact, this is true. Alabugin et al. claimed that the strongly polar O–H bonds are contracted upon the complexes of ROH (R = Me, CH₂OH, *t*-Bu) with CF₄ formation by using the MP2/6-31+G* calculations⁷. However, our calculations at the MP2/aug-cc-pVTZ theory level showed that all the O–H bonds are elongated upon these complexes formation. The O–H bonds are elongated about 0.0001, 0.0002 and 0.0002 Å, respectively, upon the complexes CH₃OH...CF₄, CH₂(OH)₂...CF₄ and *t*-BuOH...CF₄ formation. Figure 1 shows the N–H and P–H bond-length changes upon complexes NH₃...PH₃ and PH₃...NH₃ formation. The strongly polar N–H bond is elon-

TABLE I
The X-Y bond-length change (in Å; X = O, S, N, P, C, Si, H, F, Cl, Br; Y = H, Cl, Br) upon complex formation. The distance between Y and Cl⁻ is kept constant at 7.0 Å and the angle X-Y-Cl⁻ is kept constant at 180°

Dimer	$\Delta r_{O(S)-H}$	Dimer	$\Delta r_{N(P)-H}$	Dimer	Δr_{C-H}	Dimer	Δr_{C-Cl}
HO-H...Cl ⁻	0.0014	H ₂ N-H...Cl ⁻	0.0011	H ₃ C-H...Cl ⁻	-0.0004	H ₃ C-Cl...Cl ⁻	-0.0040
FO-H...Cl ⁻	0.0014	F ₂ N-H...Cl ⁻	0.0003	H ₂ FC-H...Cl ⁻	-0.0008	H ₂ FC-Cl...Cl ⁻	-0.0096
HS-H...Cl ⁻	0.0008	H ₂ P-H...Cl ⁻	-0.0016	HF ₂ C-H...Cl ⁻	-0.0011	HF ₂ C-Cl...Cl ⁻	-0.0102
FS-H...Cl ⁻	-0.0005	F ₂ P-H...Cl ⁻	-0.0045	F ₃ C-H...Cl ⁻	-0.0010	F ₃ C-Cl...Cl ⁻	-0.0114
HO-H...H ⁺	-0.0011	OH-H...Cl ⁻	-0.0025	FOC-H...Cl ⁻	-0.0008	HO-Cl...Cl ⁻	0.0045
Dimer	Δr_{X-H}	Dimer	Δr_{C-H}	Dimer	Δr_{C-Br}	Dimer	Δr_{Si-H}
H-H...Cl ⁻	0.0004	NC-H...Cl ⁻	0.0013	H ₃ C-Br...Cl ⁻	-0.0030	H ₃ Si-H...Cl ⁻	-0.0046
F-H...Cl ⁻	0.0015	H ₂ CHC-H...Cl ⁻	-0.0003	H ₂ FC-Br...Cl ⁻	-0.0075	H ₂ FSi-H...Cl ⁻	-0.0042
Cl-H...Cl ⁻	0.0019	H ₅ C ₆ -H...Cl ⁻	-0.0004	HF ₂ C-Br...Cl ⁻	-0.0105	HF ₂ Si-H...Cl ⁻	-0.0043
Br-H...Cl ⁻	0.0015	HOC-H...Cl ⁻	-0.0021	F ₃ C-Br...Cl ⁻	-0.0095	F ₃ Si-H...Cl ⁻	-0.0032

gated about 0.0003 Å upon complex $\text{NH}_3 \cdots \text{PH}_3$ formation and the weakly polar P–H bond is contracted about 0.0009 Å upon complex $\text{PH}_3 \cdots \text{NH}_3$ formation. Again, it is proved that the electrostatic interaction forces the strongly polar bond elongation and causes the weakly polar bond contraction.

The Role of the Charge-Transfer Interaction in the Bond-Length Change upon Molecule Complexation

Table II lists the C–Y bond-length change and the charge-transfer $E(2)$ stabilisation energy for various Y–Cl[–] distances of the $\text{F}_n\text{C–Y} \cdots \text{Cl}^-$ complexes. The formation of these complexes is associated with the $\text{LP}(\text{Cl}^-) \rightarrow \sigma^*(\text{C–Y})$ charge transfer. As shown in Table II, at the long Y–Cl[–] distance (7.0 Å), there are no charge-transfer ($E(2) = 0$) or other short-range interactions. When the Y–Cl[–] distance decreases to 3.0 Å, the situation is different and the role of the charge-transfer interaction is absolutely crucial to the C–Y bond-length change upon complex formation. It results in the lengthening of the C–H bond in $\text{H}_3\text{CH} \cdots \text{Cl}^-$, the C–Cl bond in $\text{H}_3\text{CCl} \cdots \text{Cl}^-$ or the C–Br bond in $\text{H}_3\text{CBr} \cdots \text{Cl}^-$ upon complex formation. Table II shows that the value of the elongation is proportional to the $E(2)$ energy. Other C–Y bonds are, however, still contracted upon complex formation because of the stronger electrostatic attractive interaction. The values of $E(2)$ in the last column of Table II indicate that the F substitution increases the electron-accepting ability of the C–Y σ^* antibonding orbital. This increase together with the

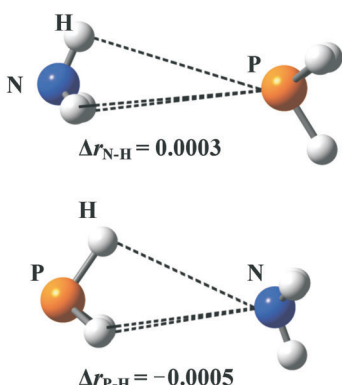


FIG. 1
The N–H and P–H bond-length changes (in Å) upon complexes $\text{NH}_3 \cdots \text{PH}_3$ and $\text{PH}_3 \cdots \text{NH}_3$ formation

electrostatic attractive interaction explain why the C–H and C–Br bonds are elongated upon the formation of the $\text{F}_3\text{CH}\cdots\text{Cl}^-$ and $\text{F}_3\text{CBr}\cdots\text{Cl}^-$ complexes⁵.

The strength of a covalent bond depends on the attraction of the nuclei for the shared electrons; therefore, the greater the orbital overlap, the stronger the bond. The overlap of two atomic orbitals depends upon the symmetry of the orbitals, the distance between the orbitals, the spatial extent of the orbitals, and the energy difference between the orbitals. Similarly, for the overlap between the X–Y σ^* antibonding orbital and the electron-rich orbital of Z, the principle of maximum overlap and energy match still work. It means, the greater the orbital overlap and the closer the energy match, the stronger the charge-transfer interaction and the longer the X–Y bond.

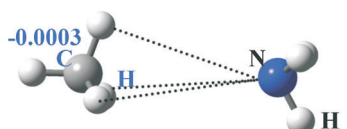
Figure 2 illustrates the C–H bond-length change upon the $\text{CH}_4\cdots\text{NH}_3$ complex formation. The three C–H bonds in the upper configuration are all contracted, whereas the C–H bond in the lower configuration shows elongation. Similarly, Tian et al. reported that shortening of the C–H bonds was

TABLE II

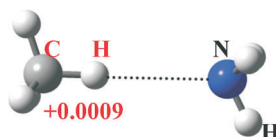
The C–Y bond-length change (in Å) and the second-order stabilisation energy $E(2)$ (in kcal/mol) of the $\text{LP}(\text{Cl}^-) \rightarrow \sigma^*(\text{C–Y})$ interaction at various Y–Cl[−] distances (in Å) upon $\text{F}_n\text{C–Y}\cdots\text{Cl}^-$ complex formation (Y = H, Cl, Br; n = 0–3). The angle C–Y–Cl[−] is kept constant at 180°

Complex	$R_{(\text{Y}\cdots\text{Cl}^-)} = 7.0$		$R_{(\text{Y}\cdots\text{Cl}^-)} = 3.0$	
	$\Delta r_{\text{C–Y}}$	$E(2)$	$\Delta r_{\text{C–Y}}$	$E(2)$
$\text{H}_3\text{CH}\cdots\text{Cl}^-$	−0.0004	0.00	+0.0023	1.07
$\text{FH}_2\text{CH}\cdots\text{Cl}^-$	−0.0008	0.00	−0.0004	1.35
$\text{F}_2\text{HCH}\cdots\text{Cl}^-$	−0.0011	0.00	−0.0020	1.69
$\text{F}_3\text{CH}\cdots\text{Cl}^-$	−0.0010	0.00	−0.0017	2.19
$\text{H}_3\text{CCl}\cdots\text{Cl}^-$	−0.0040	0.00	+0.0026	6.25
$\text{FH}_2\text{CCl}\cdots\text{Cl}^-$	−0.0096	0.00	−0.0140	6.34
$\text{F}_2\text{HCCl}\cdots\text{Cl}^-$	−0.0102	0.00	−0.0224	6.69
$\text{F}_3\text{CCl}\cdots\text{Cl}^-$	−0.0114	0.00	−0.0235	7.34
$\text{H}_3\text{CBr}\cdots\text{Cl}^-$	−0.0030	0.00	+0.0182	11.56
$\text{FH}_2\text{CBr}\cdots\text{Cl}^-$	−0.0075	0.00	−0.0009	11.84
$\text{F}_2\text{HCBr}\cdots\text{Cl}^-$	−0.0105	0.00	−0.0117	12.58
$\text{F}_3\text{CBr}\cdots\text{Cl}^-$	−0.0095	0.00	−0.0062	13.96

found in the $\text{XCH}_3\cdots\text{NH}_3$ ($\text{X} = \text{F, Cl, Br, I}$) complexes and lengthening of the C–H bonds was found in the $\text{X}_3\text{CH}\cdots\text{NH}_3$ ($\text{X} = \text{F, Cl, Br, I}$) complexes⁸. In fact, the C–H bond-length change displayed in Fig. 2 is a general trend whatever the electron donor is. For example, Hobza et al. also found that the C–H bonds in the anionic $\text{Z}\cdots\text{H}_3\text{CX}$ ($\text{Z} = \text{Cl, I}$; $\text{X} = \text{Br, I}$) complexes contract upon complex formation while the C–H bonds in the $\text{Z}^-\cdots\text{HCH}_3$ ($\text{Z} = \text{Cl, I}$) anion–molecule complexes are elongated³. Evidently, the different bond-length change can be explained by using the above-mentioned principle of maximum overlap. In the upper configurations of the complex, the three C–H σ^* antibonding orbitals do not all point to the nitrogen lone-pair orbital. The overlap between the three C–H σ^* antibonding orbitals and the nitrogen lone-pair orbital is thus rather small ($E(2) = 0.14 \text{ kcal/mol}$). Consequently, the electron density transfer to the C–H σ^* antibonding orbital is only of minor importance, and it is the electrostatic attractive interaction that causes the C–H bond contraction. On the contrary, in the lower configurations of the complex, the C–H σ^* antibonding orbital points to the nitrogen lone-pair orbital, and an efficient overlap between them is expected ($E(2) = 0.86 \text{ kcal/mol}$). Consequently, the electron-density transfer to the C–H σ^* antibonding orbital is responsible for the elongation of the C–H bond in the lower configurations of the complex. Let us mention here that, in a variety of complexes involving C–H…O interaction, the C–H bonds were always found to be contracted, because the C–H σ^* antibonding orbital cannot overlap with the oxygen lone pairs favourably⁶.



Contraction of the C–H bonds



Elongation of the C–H bond

FIG. 2

The C–H bond-length change (in Å) in the two configurations of the $\text{CH}_4\cdots\text{NH}_3$ complex determined by the overlap between the C–H σ^* antibonding orbital and the nitrogen lone-pair orbital

Orbital energy match also plays an important role in the bond-length change of the less polar bond upon molecule complexation. Table III collects the energies of the low unoccupied molecular orbitals of some typical proton donors for the blue-shifting hydrogen bonds and halogen donors for the blue-shifting halogen bonds. In each proton donors except CH_4 , the $\text{C}-\text{H} \sigma^*$ antibonding orbital is not the lowest unoccupied molecular orbital. This means that the electron density transfers from the electron-rich orbital of the proton acceptor to other lower unoccupied molecular orbital not to the $\text{C}-\text{H} \sigma^*$ antibonding orbital of the proton donor. It is indicated that the charge transfer plays a dominant role for the bond-length change of the hydrogen bond. For the typical halogen donors of the blue-shifting halogen

TABLE III
The energies (a.u.) of the low unoccupied molecular orbitals of some selected monomers

Monomer	Energies of the lowest unoccupied molecular orbitals	Monomer	Energies of the lowest unoccupied molecular orbitals
HNO	BD*(1) N–O: 0.1256 BD*(1) N–H: 0.5414	CH_4	BD*(1) C–H: 0.6384
HCHO	BD*(1) C–O: 0.1872 BD*(1) C–H: 0.5617	CFH_3	BD*(1) C–F: 0.4979 BD*(1) C–H: 0.5932
FCHO	BD*(1) C–O: 0.1657 BD*(1) C–F: 0.4870 BD*(1) C–H: 0.5257	CF_2H_2	BD*(1) C–F: 0.5098 BD*(1) C–H: 0.5529
CH_3CHO	BD*(1) C–O: 0.21007 BD*(1) C–H: 0.56221	CF_3H	BD*(1) C–F: 0.5169 BD*(1) C–H: 0.5191
CH_3Cl	BD*(1) C–Cl: 0.3396 BD*(1) C–H: 0.5962	CH_3Br	BD*(1) C–Br: 0.2733 BD*(1) C–H: 0.6047
CFH_2Cl	BD*(1) C–Cl: 0.3177 BD*(1) C–F: 0.4793 BD*(1) C–H: 0.5528	CFH_2Br	BD*(1) C–Br: 0.2505 BD*(1) C–F: 0.4738 BD*(1) C–H: 0.5629
CF_2HCl	BD*(1) C–Cl: 0.2946 BD*(1) C–F: 0.4861 BD*(1) C–H: 0.5163	CF_2HBr	BD*(1) C–Br: 0.2267 BD*(1) C–F: 0.4821 BD*(1) C–H: 0.5254
CF_3Cl	BD*(1) C–Cl: 0.2876 BD*(1) C–F: 0.4868	CF_3Br	BD*(1) C–Br: 0.2066 BD*(1) C–F: 0.4832

bonds in Table III, the case is totally different. All the C–Cl(Br) σ^* anti-bonding orbitals are the lowest unoccupied molecular orbitals, which indicates that the electrostatic interaction plays a dominant role for the bond-length change of the halogen bond. From these discussions, we can see that the nature of the bond-length change for the hydrogen bond is a little different from that for the halogen bond.

For the bond-length change upon molecule complexation, an interesting question appears: is it possible to predict the largest contraction of the X–Y bond upon molecule complexation? The answer is yes! First, for the electron acceptor, we should select the one with the largest X–Y contraction in the electric field of the electron donor. Table II shows that F_3CCl is the best choice. Second, a very strong electron donor should be selected. Divalent and trivalent anions always result in the rupture of the X–Y bond upon complex formation, so only monovalent anions can be considered. At the same time, according to the principle of closer energy match, we should select the one with the lowest energy of the lone electron pair. Note that a poor energy match will lead to a weak charge-transfer interaction. Table IV lists some common anions along with their respective orbital energies of lone electron pairs. For the anions F^- , Cl^- , Br^- , OH^- or SH^- , the orbital energy of LP(1) is lower than that of the other lone pairs. In the case of spheric anions like F^- , Cl^- and Br^- the higher-lying LP(2), LP(3) or LP(4) orbital is systematically engaged in charge-transfer process ($\text{LP} \rightarrow \sigma^*$). Only in the case of OH^- and SH^- anions we can change the situation and utilize also

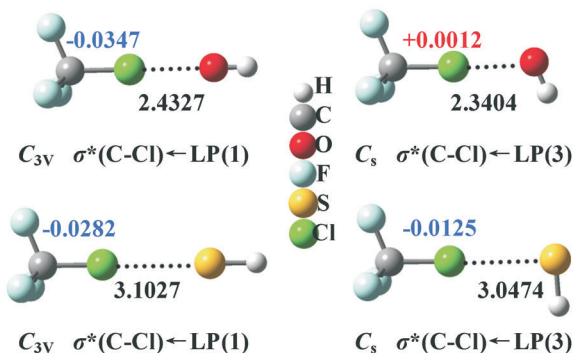


FIG. 3

The C–Cl bond-length change (in Å) and the distance between the Cl and O(S) (in Å) of the $\text{F}_3\text{CCl}\cdots\text{OH}^-$ and $\text{F}_3\text{CCl}\cdots\text{SH}^-$ complexes

TABLE IV
The energy (a.u.) of the lone-pair orbital in some common anions

Electron donor	Orbital energy	Electron donor	Orbital energy
F ⁻	LP(1): -1.0760	CN ⁻	LP(1) C: -0.3063
	LP(2): -0.1810		LP(1) N: -0.4532
	LP(3): -0.1810		LP(1) O: -0.7721
	LP(4): -0.1810		LP(2) O: -0.1061
Cl ⁻	LP(1): -0.7335	OH ⁻	LP(3) O: -0.1061
	LP(2): -0.1503		LP(1) S: -0.6363
	LP(3): -0.1503		LP(2) S: -0.0991
	LP(4): -0.1503		LP(3) S: -0.0991
Br ⁻	LP(1): -0.6860	SH ⁻	
	LP(2): -0.1393		
	LP(3): -0.1393		
	LP(4): -0.1393		
H ⁻	LP(1): -0.0457		

the lower-lying lone pair orbital LP(1). Figure 3 shows the overlaps between the C-Cl σ^* antibonding orbital and the different lone-pair orbitals of O or S. As expected, when the lone-pair orbital with the lower energy, (LP(1)) is involved in the overlap (linear approach of HX; left side of Fig. 3), the contraction of the C-Cl bond is more obvious. In the case of non-linear approach (right side of Fig. 3) the contraction is smaller and in the case of OH⁻ even the elongation occurred. When the distance between Cl and S in the C_s configuration of the complex F₃CCl₂...SH⁻ is longer the overlap between the C-Cl σ^* antibonding orbital and LP(2) (or LP(3)) of S is smaller and contraction of the C-Cl bond upon complex formation resulted. This is despite the fact that the energy of LP(2) (or LP(3)) of S is relatively high (higher than that of O). Consequently, we can predict that the contraction of the C-Cl bond in the C_{3v} configuration of the complex F₃CCl₂...OH⁻ is the largest among the complexes considered here. Our prediction is confirmed by a search in the database (Table V).

TABLE V
The database of the bond-length change (in Å) upon complex formation calculated at the MP2/aug-cc-pVTZ theory level

Complex	R_{X-Cl}	Δr_{X-Cl}	Complex	R_{X-Cl}	Δr_{X-Cl}	Complex	R_{X-Cl}	Δr_{X-Cl}
$F_2BCl...F^-$	1.7140	-0.0278	$F_3CCl...F^-$	1.7329	-0.0187	$F_3SiCl...F^-$	1.9815	-0.0271
$F_2BCl...Cl^-$	1.7183	-0.0235	$F_3CCl...Cl^-$	1.7290	-0.0225	$F_3SiCl...Cl^-$	1.9835	-0.0251
$F_2BCl...Br^-$	1.7198	-0.0220	$F_3CCl...Br^-$	1.7319	-0.0197	$F_3SiCl...Br^-$	1.9845	-0.0241
$F_2BBr...F^-$	1.8781	-0.0149	$F_3CBr...F^-$	1.9296	0.0194	$F_3SiBr...F^-$	2.1534	-0.0083
$F_2BBr...Cl^-$	1.8748	-0.0182	$F_3CBr...Cl^-$	1.9126	0.0024	$F_3SiBr...Cl^-$	2.1449	-0.0168
$F_2BBr...Br^-$	1.8758	-0.0172	$F_3CBr...Br^-$	1.9131	0.0029	$F_3SiBr...Br^-$	2.1454	-0.0163
$F_3GeCl...F^-$	2.0755	-0.0029	$F_3CCl...NC^-$	1.7273	-0.0242	$F_3CCl...CN^-$	1.7328	-0.0188
$F_3GeCl...Cl^-$	2.0637	-0.0147	$F_3SiCl...NC^-$	1.9840	-0.0246	$F_3SiCl...CN^-$	1.9851	-0.0234
$F_3GeCl...Br^-$	2.0638	-0.0146	$F_3CBr...NC^-$	1.9069	-0.0033	$F_3CBr...CN^-$	1.9328	0.0225
$F_3GeBr...F^-$	2.2621	0.0407	$F_3SiBr...NC^-$	2.1444	-0.0173	$F_3SiBr...CN^-$	2.1488	-0.0129
$F_3GeBr...Cl^-$	2.2308	0.0093						
$F_3GeBr...Br^-$	2.2297	0.0082						
$F_3CCl...OH^-$	1.7168	-0.0347	$F_3CCl...SH^-$	1.7233	-0.0282	$F_3CCl...H^-$		
$F_3SiCl...OH^-$	1.9759	-0.0326	$F_3SiCl...SH^-$	1.9814	-0.0272	$F_3SiCl...H^-$	1.9918	-0.0167
$F_3CBr...OH^-$	1.8979	-0.0124	$F_3CBr...SH^-$	1.8906	-0.0196	$F_3CBr...H^-$		
$F_3SiBr...OH^-$	2.1377	-0.0240	$F_3SiBr...SH^-$	2.1370	-0.0247	$F_3SiBr...H^-$		

CONCLUSIONS

The nature of the bond-length change upon complex formation has been investigated theoretically. The following conclusions can be drawn from this study: (i) For the electron-rich, more polar X–Y bonds, both the electrostatic attractive interaction and charge-transfer interaction result in their elongation. For less polar, electron-poor X–Y bonds, the electrostatic attractive interactions force them to contract, whereas the charge-transfer interaction causes them to elongate, and the net X–Y bond-length change is determined by the balance between the electrostatic attractive interaction and the charge-transfer interaction. (ii) The charge-transfer plays a dominant role for the bond-length change of the hydrogen bond whereas for the bond-length change of the halogen bond the electrostatic interaction plays a dominant role. (iii) Employing the simple “electrostatic interaction plus charge-transfer interaction” explanation, we also predicted and confirmed the contraction of the C–Cl bond in the C_{3v} configuration of the complex $F_3CCl\cdots OH^-$ is the largest among the complexes considered in the present study.

This project was supported by the Scientific Research Foundation for the Returned Overseas Chinese Scholars, Ministry of Education of China and the National Natural Science Foundation of China (Grant No. 20872057).

REFERENCES

1. Hobza P., Špirko V., Selzle H. L., Schlag E. W.: *J. Phys. Chem. A* **1998**, *102*, 2501.
2. Hobza P., Havlas Z.: *Chem. Phys. Lett.* **1999**, *303*, 447.
3. Hobza P., Havlas Z.: *Chem. Rev.* **2000**, *100*, 4253.
4. Li X., Liu L., Schlegel H. B.: *J. Am. Chem. Soc.* **2002**, *124*, 9639.
5. Hermansson K.: *J. Phys. Chem. A* **2002**, *106*, 4695.
6. Delanoye S. N., Herrebout W. A., van der Veken B. J.: *J. Am. Chem. Soc.* **2002**, *124*, 7490.
7. Alabugin I. V., Manoharan M., Peabody S., Weinhold F.: *J. Am. Chem. Soc.* **2003**, *125*, 5973.
8. Wang X., Zhou G., Tian A. M., Wong N. B.: *J. Mol. Struct. (THEOCHEM)* **2005**, *718*, 1.
9. Lu P., Liu G., Li J.: *J. Mol. Struct. (THEOCHEM)* **2005**, *723*, 95.
10. McDowell S. A. C., Buckingham A. D.: *J. Am. Chem. Soc.* **2005**, *127*, 15515.
11. Joseph J., Jemmis E. D.: *J. Am. Chem. Soc.* **2007**, *129*, 4620.
12. Wang W. Z., Hobza P.: *Collect. Czech. Chem. Commun.* **2008**, *73*, 862.
13. Trung N. T., Hue T. T., Nguyen M. T.: *J. Phys. Chem. A* **2009**, *113*, 3245.
14. Karpfen A.: *Struct. Bonding* **2008**, *126*, 1.
15. Wang W. Z., Wong N. B., Zheng W. X., Tian A. M.: *J. Phys. Chem. A* **2004**, *108*, 1799.
16. Wang W. Z., Hobza P.: *J. Phys. Chem. A* **2008**, *112*, 4114.
17. Feng Y., Liu L., Wang J. T., Li X. S., Guo Q. X.: *Chem. Commun.* **2004**, *88*.

18. Metrangolo P., Resnati G.: *Science* **2008**, *321*, 918.
19. Frisch M. J., Trucks G. W., Schlegel H. B., Scuseria G. E., Robb M. A., Cheeseman J. R., Montgomery J. A., Jr., Vreven T., Kudin K. N., Burant J. C., Millam J. M., Iyengar S. S., Tomasi J., Barone V., Mennucci B., Cossi M., Scalmani G., Rega N., Petersson G. A., Nakatsuji H., Hada M., Ehara M., Toyota K., Fukuda R., Hasegawa J., Ishida M., Nakajima T., Honda Y., Kitao O., Nakai H., Klene M., Li X., Knox J. E., Hratchian H. P., Cross J. B., Adamo C., Jaramillo J., Gomperts R., Stratmann R. E., Yazyev O., Austin A. J., Cammi R., Pomelli C., Ochterski J. W., Ayala P. Y., Morokuma K., Voth G. A., Salvador P., Dannenberg J. J., Zakrzewski V. G., Dapprich S., Daniels A. D., Strain M. C., Farkas O., Malick D. K., Rabuck A. D., Raghavachari K., Foresman J. B., Ortiz J. V., Cui Q., Baboul A. G., Clifford S., Cioslowski J., Stefanov B. B., Liu G., Liashenko A., Piskorz P., Komaromi I., Martin R. L., Fox D. J., Keith T., Al-Laham M. A., Peng C. Y., Nanayakkara A., Challacombe M., Gill P. M. W., Johnson B., Chen W., Wong M. W., Gonzalez C., Pople J. A.: *Gaussian 03*, Revision C.02. Gaussian, Inc., Wallingford (CT) 2004.
20. Reed A. E., Curitss L. A., Weinhold F.: *Chem. Rev.* **1988**, *88*, 899.
21. Shameema O., Ramachandran C. N., Sathyamurthy N.: *J. Phys. Chem. A* **2006**, *110*, 2.
22. Wang W. Z., Zhang Y., Huang K. X.: *Chem. Phys. Lett.* **2005**, *405*, 425.